

# Numerical and Theoretical Studies of Noise Effects in the Kauffman Model

X. Qu,<sup>1</sup> M. Aldana,<sup>1</sup> and Leo P. Kadanoff<sup>1</sup>

*Received May 14, 2002; accepted July 11, 2002*

---

In this work we analyze the stochastic dynamics of the Kauffman model evolving under the influence of noise. By considering the average crossing time between two distinct trajectories, we show that different Kauffman models exhibit a similar kind of behavior, even when the structure of their basins of attraction is quite different. This can be considered as a robust property of these models. We present numerical results for the full range of noise level and obtain approximate analytic expressions for the above crossing time as a function of the noise in the limit cases of small and large noise levels.

---

**KEY WORDS:** Kauffman model; noise; crossing time; robustness.

## 1. INTRODUCTION

The Kauffman model (or  $N$ - $K$  model) describes the dynamics of a network of  $N$  Boolean spins, each controlled by  $K$  other spins through a binary function. It was first proposed by S. A. Kauffman in 1969<sup>(1)</sup> as a model for cell differentiation and genetic networks. Since then, its application has been extended to many other fields in physics, biology, computational and social sciences. During the past few decades, most of the work done on Kauffman models has been dedicated to the study of the configuration space structure, the length and number of cycles, the size of basins of attraction, and the phase transition between ordered and disordered phases (for references, see ref. 2). These properties are obtained by considering the deterministic dynamics of the system, which is well known by now. However, those studies have shown that some of the generic properties of the Kauffman model are far from being robust. The non-robustness of the

---

<sup>1</sup> The James Franck Institute, The University of Chicago, 5640 South Ellis Avenue, Chicago, Illinois 60637; e-mail: quxh@uchicago.edu

deterministic dynamics is reflected, for example, in the fact that by slightly changing a given initial configuration of spins, the system may “jump” from one basin of attraction to a very different one. On the other hand, due to the exponential growth of the state space with  $N$ , it is often necessary to thoroughly probe the state space in order to determine a generic property of the system, such as the mean number of different basins of attraction or the mean cycle length. Actually, it has recently been shown that a systematic bias due to an under-sampling of the state space can be present in some of the results reported in the literature during the last 30 years.<sup>(3)</sup> Therefore it is valuable to find a method which reveals the robust properties of the Kauffman model.

Real networks are always subjected to external fluctuations. Consequently, the relevant properties characterizing the network should exhibit a certain degree of robustness to external perturbations. In 1989, both Miranda *et al.*<sup>(4)</sup> and Golinelli *et al.*<sup>(5)</sup> analyzed the stochastic dynamics of the Kauffman model in the case in which an external noisy signal is present. In this work we extend the study of the stochastic dynamics of the Kauffman network with noise, by performing more accurate numerical simulations as well as analytic calculations. We focus our attention on the time it takes for two trajectories, starting out from different initial conditions, to cross. We consider two cases. First the situation in which each one of the  $N$  spins is determined by  $K$  other spins chosen randomly from everywhere in the system (the Kauffman net). The second case is a  $d$ -dimensional lattice in which each spin is preferentially coupled to its immediate neighbors. As we will see, both models exhibit qualitatively similar behavior.

In Section 2, we introduce the Kauffman model with deterministic and stochastic dynamics. In Section 3 we describe our numerical results for both Kauffman nets and lattices. In Section 4, we study closely the behavior of these models in the limits of small and large noise. We summarize this work in Section 5 with a brief discussion of the results.

## 2. THE KAUFFMAN MODEL

### 2.1. Deterministic Dynamics

A Kauffman model consists of  $N$  Boolean spins  $\{S_1, S_2, \dots, S_N\}$  with  $S_i$  being either zero or one. The value of each spin  $S_i$  at time  $t+1$  is determined by the values of  $K$  other spins  $S_{i_1}, S_{i_2}, \dots, S_{i_K}$ , which are called the *controlling elements* for spin  $S_i$ . (The number  $K$  is called the *connectivity* of the system.) Once the connections in the system are established, each spin  $S_i$  is assigned with a Boolean function  $f_i$  of its  $K$  controlling elements.

A realization of the Kauffman model consists of the set of connections and Boolean functions assigned to every spin. The dynamics of the network is then given by

$$S_i(t+1) = f_i(S_{i_1}(t), S_{i_2}(t), \dots, S_{i_K}(t)) \quad \text{for } i = 1, \dots, N. \quad (1)$$

For convenience, we will denote by  $\Sigma_t$  the state of the system at time  $t$ :

$$\Sigma_t = \{S_1(t), S_2(t), \dots, S_N(t)\}.$$

In different Kauffman models, the assignments of the  $K$  controlling spins  $S_{i_1}, S_{i_2}, \dots, S_{i_K}$  of each spin  $S_i$  and the dynamic rules  $f_i$ , are different. In *Kauffman nets*, the controlling elements of  $S_i$  are assigned randomly, whereas in a *Kauffman lattice* they are chosen only among its nearest neighbors. The dynamic rules  $f_i$  are chosen randomly in such a way that its two possible outcomes, 0 and 1, occur with probability  $\rho$  and  $1 - \rho$  respectively. If the realization of the network is time-independent, the network is called *quenched*, while if either the set of connections or the set of Boolean functions  $f_i$  are re-assigned at every time step, the network is termed *annealed*.

Annealed models are more convenient for theoretical studies than quenched models. For example, by using the annealed approximation it has been shown analytically that Kauffman nets exhibit three different phases: frozen, critical and chaotic, depending upon the values of the parameters  $K$  and  $\rho$ .<sup>(6)</sup> The critical value of the connectivity is given by  $K_c = [2\rho(1-\rho)]^{-1}$ . For  $K < K_c$  the system is in the frozen phase, whereas if  $K > K_c$  it is in the chaotic phase. Throughout this work we will use  $\rho = 1/2$ , for which  $K_c = 2$ .

But for most real cases (neural networks, genetic networks, etc.), quenched models will be more appropriate since in real networks neither the connections nor the interactions between the elements change randomly at every moment. However, it has been shown that in the limit  $N \rightarrow \infty$ , both the quenched and the annealed Kauffman nets are exactly equivalent with respect to the evolution of the overlap between different configurations, although not with respect to the configurations themselves.<sup>(7-9)</sup> In this paper, our main focus is on quenched Kauffman nets and lattices.

Due to the finite size of the system, there are a finite number of possible configurations, to wit  $\Omega = 2^N$ . Therefore, starting out with an initial configuration, the system will eventually fall into a previously visited state, after which the same sequence of states repeatedly occurs again. The state space breaks up into a multitude of cycles (or attractors). The totality of points which end up in the same attractor represents its *basin of attraction*.

## 2.2. Stochastic Dynamics

There are different ways of introducing noise into Kauffman models and they reveal different features of the configuration space of the model. Following Miranda and Parga,<sup>(4)</sup> we introduced noise in the following way:

$$S_i(t+1) = \begin{cases} f_i(S_{i_1}(t), S_{i_2}(t), \dots, S_{i_K}(t)) & \text{with probability } 1-r, \\ 1 - f_i(S_{i_1}(t), S_{i_2}(t), \dots, S_{i_K}(t)) & \text{with probability } r. \end{cases} \quad (2)$$

In this way, every spin  $S_i$  has a probability  $r$  of violating the deterministic rule (1). We will say that an  $n$ -spin flip event has occurred at a particular time step, if  $n$  spins violated the deterministic rule in this time step. Notice that this stochastic dynamic rule has a symmetry about the point  $r = 0.5$ . For  $r > 0.5$ , if we make a substitution  $f_i \rightarrow 1 - f_i$ , the rule becomes identical with the case of  $1 - r$ . Since the Boolean functions  $f_i$  are assigned randomly,  $f_i$  and  $1 - f_i$  are equally likely to appear in a particular realization of the model. After averaging over different realizations, the cases with probabilities  $r$  and  $1 - r$  are indeed identical. Due to this symmetry in the stochastic dynamical rule (2), we only need to consider the case  $r \in [0, 0.5]$ . Note that for the particular value  $r = 0.5$ ,  $S_i(t+1)$  is equally likely to be zero or one independently of the value of  $f_i$ .

In the presence of noise, the concept of ‘‘attractor’’ does not hold any more, since as the system evolves, there is a non-zero probability of ‘‘jumping’’ to a different attractor, and consequently every point in the state space can be reached from any initial condition. In this sense, the ‘‘boundaries’’ between different attractors become more diffuse as the level of noise increases.<sup>(10)</sup> However, we shall argue that the system has a sort of effective attractor even in the presence of noise, specifically when  $r$  is large.

One of the interesting things to study is the time it takes for two trajectories to cross. Suppose that we start with two different initial configurations,  $\Sigma_0$  and  $\tilde{\Sigma}_0$ , and let them evolve according to (2), noting all the configurations produced:

$$\begin{aligned} \Sigma_0 &\rightarrow \Sigma_1 \rightarrow \Sigma_2 \rightarrow \dots \rightarrow \Sigma_\tau \\ \tilde{\Sigma}_0 &\rightarrow \tilde{\Sigma}_1 \rightarrow \tilde{\Sigma}_2 \rightarrow \dots \rightarrow \tilde{\Sigma}_\tau \end{aligned}$$

The crossing time  $\tau$  is then defined as the time for which either one of the trajectories coincides for the first time with a configuration previously visited by the other trajectory. For example, when  $\tilde{\Sigma}_\tau$  is equal to any of the configurations  $\Sigma_0, \Sigma_1, \Sigma_2, \dots, \Sigma_\tau$ . Two important cases have to be distinguished, when  $\Sigma_0$  and  $\tilde{\Sigma}_0$  belong to the same basin of attraction, and when they belong to different basins of attraction. For those cases we will denote the crossing time by  $\tau_s$  and  $\tau_d$ , respectively.

Miranda and Parga examined the behavior of the system by considering only the attractors with largest and next-largest basins of attraction. They then showed that for small values of  $r$ , the behavior of  $\tau_s$  and  $\tau_d$  are very different. At  $r = 0$ , two trajectories from the same basin will cross in a time comparable with the sum of two times: first, the transient time required to enter the attractor, and second, the length of the attractor itself. Conversely, two trajectories starting out from different basins will never cross. On the other hand, they found that for sufficiently large values of  $r$ , the crossing time became independent of the starting point. It did not matter where the two trajectories start, the two basins merge into a sort of effective attractor and the trajectory bounces around within that subset of the system-states. For these larger values of  $r$ , the observed effective basin size increased with  $r$ . From this, they drew the conclusion that the disappearance of basins of attraction with the increase of  $r$  is a sort of hierarchical process in the sense that in a finite period of time, the portion of the whole state space explored by a trajectory starting out from a given basin of attraction increases with  $r$ . Complete randomness is achieved at  $r = 0.5$ , where the trajectory explores the entire state space.

As we will see, our simulation will show the same general behavior as described by Miranda and Parga. But we shall explore the behavior in more detail, showing the crossing time for the whole range of values of  $r$  and  $K$ .

### 3. NUMERICAL RESULTS

Kauffman nets and Kauffman lattices differ in the structure of their basins of attraction. One would expect this difference to be reflected in the response of these models to the influence of noise. For random realizations of the coupling functions  $f_i$ , what determines the basin structure is the connectivity  $K$ . Therefore, we will first analyze separately the cases with large  $K$  (chaotic phase) and small  $K$  (ordered phase).

We will partially follow Miranda and Parga's approach in that we compute the average crossing time  $\tau_s$  by using two initial configurations,  $\Sigma_0$  and  $\tilde{\Sigma}_0$ , in the largest basin of attraction. For the average crossing time  $\tau_d$ , we pick one starting configuration in the largest basin and the other in the next largest one. The reasons to choose only the two largest basins of attraction will be clear in what follows.

#### 3.1. Kauffman Models with Large $K$

We want first to characterize the structure of the basins of attraction. One way of doing it is by computing the distribution of basin-sizes  $W(n)$ ,

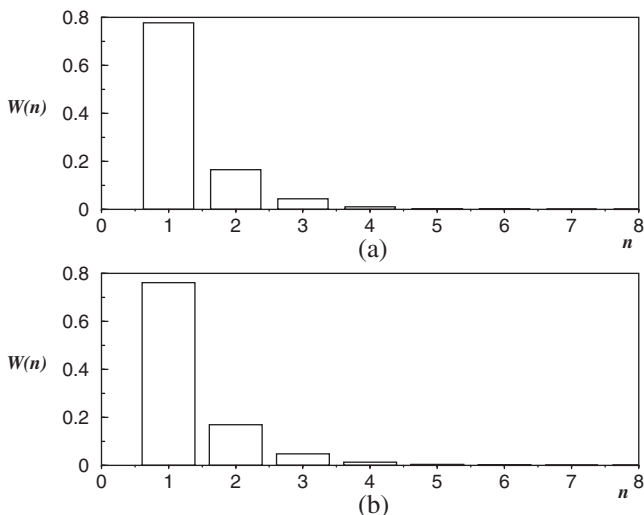


Fig. 1. Distribution  $W(n)$  of basin-sizes for: (a) the one-dimensional Kauffman lattice and (b) the Kauffman net, both with  $N = 20$  and  $K = 5$ . For the Kauffman net, the connections between spins are chosen randomly, whereas for the lattice every spin is connected to itself and to its 4 nearest neighbors (periodic boundary conditions were used). The number  $n$  in the horizontal axis corresponds to the  $n$ th largest basin in the model.

which is the fraction of the state space  $\Omega$  occupied by the  $n$ th largest basin of attraction. In Fig. 1 we show  $W(n)$  for a Kauffman net and a 1-dimensional Kauffman lattice, both with  $N = 20$  and  $K = 5$ . It can be seen from this figure that both models exhibit a very similar structure in their basins of attraction in the sense that the basin sizes are similar. It is worth mentioning that in other aspects, like orbit length or transient time,<sup>2</sup> the basins of attraction can still be very different in both models.

From Fig. 1 it also can be seen that the largest and next largest basins occupy more than 90% of the whole state space. Therefore, to a good approximation it can be assumed that the dynamics takes place mainly in these two largest basins.

Figure 2 shows the average crossing times  $\tau_s$  and  $\tau_d$  as functions of  $r$  for the Kauffman net and the 1-dimensional lattice both with  $N = 20$  and  $K = 5$  (chaotic phase). Notice that these two kinds of  $N$ - $K$  models exhibit very similar behavior under the influence of noise.

### 3.2. Kauffman Models with Small $K$

The ordered phase is characterized by  $K = 1$  and  $K = 2$ . In this section we will present the results for the minimum value of  $K$ , namely,  $K = 1$ .

<sup>2</sup> The transient time is the time it takes before a trajectory enters the stable cycle.

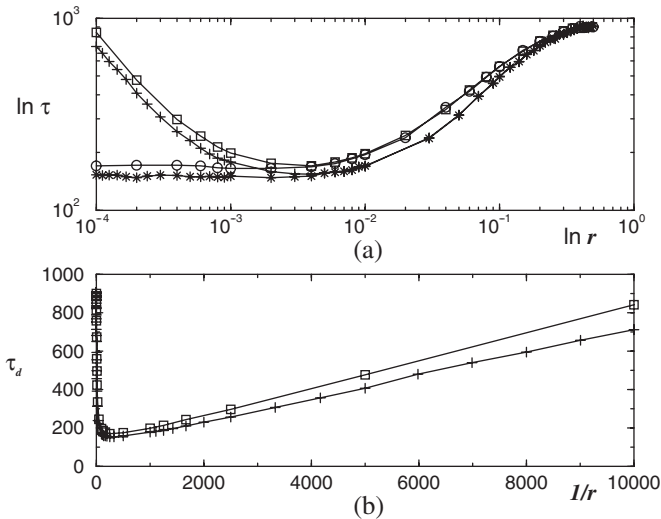


Fig. 2. Average crossing time  $\tau$  for different Kauffman models with  $N = 20$  and connectivity  $K = 5$  (chaotic phase) as a function of (a) the noise intensity  $r$  and (b) the inverse of the noise intensity. The symbols are as follows. 1-dimensional Kauffman lattice: ( $\square$ )  $\tau_d$  and ( $\circ$ )  $\tau_s$ . Kauffman net: ( $+$ )  $\tau_d$  and ( $*$ )  $\tau_s$ . Each point is the average over 4000 realizations of the model.

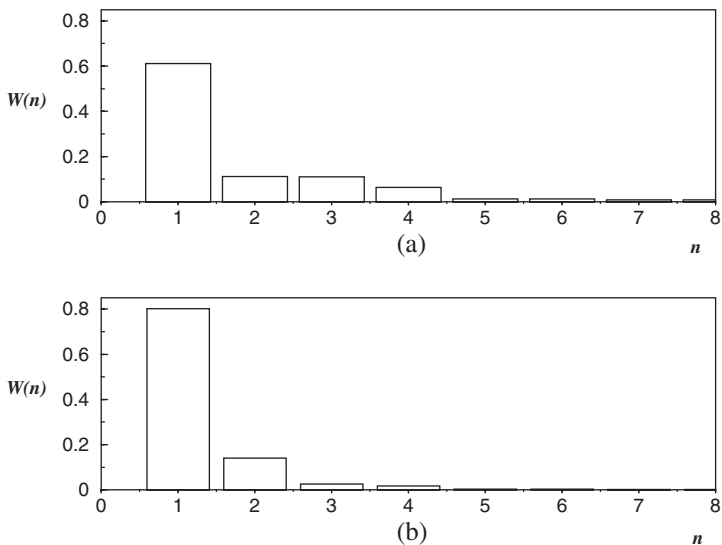


Fig. 3. Distribution  $W(n)$  of basin-sizes for: (a) the one-dimensional Kauffman lattice and (b) the Kauffman net, both with  $N = 20$  and  $K = 1$  (frozen phase). The number  $n$  in the horizontal axis has the same meaning as in Fig. 1.

In Fig. 3 we show  $W(n)$  for a Kauffman net and a 1-dimensional Kauffman lattice, both with  $N = 20$  and  $K = 1$ . The connections in the Kauffman net were, as usual, chosen randomly, whereas in the 1-dimensional lattice the node  $S_i$  was connected either to  $S_{i-1}$  or to  $S_{i+1}$  with equal probability (we use periodic boundary conditions).

From Fig. 3 it is apparent that in this case, the basin structures of the Kauffman net and the Kauffman lattice are less similar than in the chaotic phase. For the lattice, the two largest basins of attraction no longer occupy more than 90% of the whole state space, whereas in the Kauffman net they still do. However, the response to the influence of noise is mostly the same in both models, as can be seen from Fig. 4 where the crossing times  $\tau_s$  and  $\tau_d$  are plotted as functions of the noise intensity  $r$ .

### 3.3. Robust Behavior of the Crossing Time

Figures 2 and 4 show that the behavior of the different Kauffman models under the influence of noise have the following general characteristics, both in the frozen and in the chaotic phases:

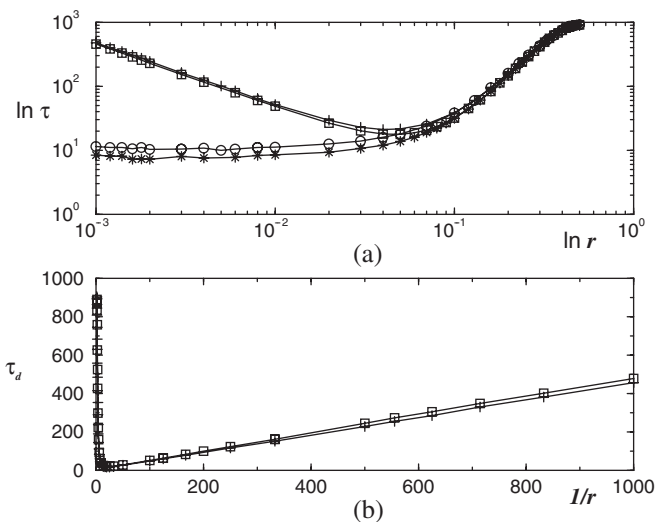


Fig. 4. Average crossing time  $\tau$  for different Kauffman models with  $N = 20$  and connectivity  $K = 1$  (frozen phase) as a function of (a) the noise intensity  $r$  and (b) the inverse of the noise intensity. The symbols are as follows. 1-dimensional Kauffman lattice: ( $\square$ )  $\tau_d$  and ( $\circ$ )  $\tau_s$ . Kauffman net: (+)  $\tau_d$  and (\*)  $\tau_s$ . Each point is the average over 4000 realizations of the model.



- For small  $r$ ,  $\tau_d$  decreases as  $1/r$  while  $\tau_s$  is nearly constant.
- For large  $r$ , both  $\tau_d$  and  $\tau_s$  increase with  $r$  and become equal at  $r = 0.5$ .
- For intermediate values of  $r$ ,  $\tau_d$  has a minimum when  $\tau_s \approx \tau_d$ .

Let us analyze separately each one of the above characteristics.

In the limit  $r \rightarrow 0$ ,  $\tau_s$  approaches a finite value  $\tau_s(0)$ , the mean crossing time for two trajectories in the largest basin of attraction in the absence of noise. This crossing time is roughly one half the average cycle length, plus one half the average transient time. The transient time and the cycle length are of the same order of magnitude, therefore  $\tau_s(0)$  is expected to be approximately equal to the mean cycle length  $\langle L \rangle$  of the largest basin of attraction (see Fig. 5a).

On the other hand,  $\tau_d$  diverges as  $r \rightarrow 0$ . The numerical data (see Figs. 2b and 4b) suggest that in this limit,  $\tau_d$  has the form

$$\tau_d \approx \frac{a(K, N)}{r} + b(K, N), \quad r \rightarrow 0. \quad (3)$$

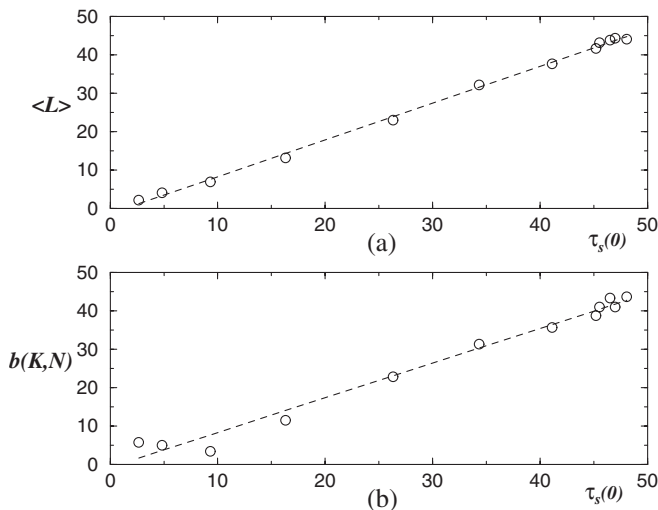


Fig. 5. (a) Plot of the mean cycle length  $\langle L \rangle$  as a function of  $\tau_s(0)$  for a Kauffman net with  $N = 12$ . Each point corresponds to a different value of  $K$ , starting with  $K = 1$  for the first point in the lower left corner of the graph and ending with  $K = 12$  for the last point in the upper right corner. The dashed line is the best linear fit to the numerical data (circles). (b) Same type of graph as before but now showing the dependence of  $b(K, N)$  on  $\tau_s(0)$ . The slopes of the dashed lines are (a)  $\sim 0.96$  and (b)  $\sim 0.90$ , which shows that  $b(K, N) \approx \tau_s(0) \approx \langle L \rangle$ .

The above divergence is due to the fact that, in the absence of noise, there is a zero probability for a trajectory to jump between different attractors. Under the deterministic dynamics, every trajectory will remain within its own basin of attraction for ever. In the next section we will see that the  $1/r$  behavior of  $\tau_d$  is a consequence of the fact that the dynamics is governed by one-spin flip events when  $r$  is small. For large values of  $K$ , the largest basin occupies almost the whole state space. Under these circumstances, every time a one-spin flip occurs, the trajectory in the next largest basin will have a finite probability of diverging very substantially from the path it would have followed in the absence of noise. That divergence will usually force the trajectory into the largest basin. In fact, for a fraction of order one of the noise events in the smaller basin, the noise will flip the trajectory into the largest one. Once the two trajectories are in the largest basin, they have a lifetime  $b(K, N)$  before they cross. This lifetime is expected to be of order one of  $\tau_s(0)$ , the typical length of the largest basin of attraction. The above can actually be seen in Fig. 5, from which it is apparent that for large  $K$ ,  $b(K, N) \approx \tau_s(0) \approx \langle L \rangle$ .

In the opposite limit  $r \rightarrow 0.5$ , the crossing times  $\tau_s$  and  $\tau_d$  become equal, which means that for high levels of noise, the barriers between different attractors become small. When  $r$  reaches its maximum value 0.5, all barriers vanish. In this case, both trajectories randomly jump from one state to another throughout the state space, and both  $\tau_s$  and  $\tau_d$  become equal to the time it takes for two random walks to cross. As derived in Section 4.2, this crossing time is the solution to the ‘‘birthday problem,’’ i.e.,

$$\tau_s = \tau_d \propto 2^{N/2} \quad (4)$$

In this way we have obtained a qualitative description of the limiting cases of Figs. 2 and 4. The one qualitative feature left to describe is the crossover from the small  $r$  to the large  $r$  behavior. As one can see from these figures, the crossover occurs when the two times  $\tau_s$  and  $\tau_d$  become roughly equal. This in turn happens when

$$r \sim a(K, N)/\tau_s(0) \sim 1/N \quad (5)$$

Thus, the minimum in  $\tau_d$  occurring between the two previous limit values of  $r$ , can be interpreted as the result of a sort of ‘‘competition’’ between the randomness in the system (coming from the presence of noise), and the barriers separating the attractors (which come from the deterministic dynamics of the system).

### 3.4. A Kauffman Model with Equal Basin-Sizes

Finally, we would like to mention that the above results are also true for Kauffman models in which all the basins of attraction have the same weight. As an example, consider a Kauffman lattice with  $N = 20$  and  $K = 1$  in which every spin is connected to itself. For  $K = 1$  there are only four Boolean functions  $f_i(S)$ : tautology  $f_i(S) = 1$ , contradiction  $f_i(S) = 0$ , identity  $f_i(S) = S$  and negation  $f_i(S) = 1 - S$ . Imagine then the very specific realization in which two of the coupling functions are identity, two are negation and all the others are either tautology or contradiction. By simple analysis, we know that for this specific model, the whole state space is composed of eight basins of attraction with equal size. Figure 6 shows the crossing time  $\tau$  as a function of  $r$  for this particular model. Since in this case all the basins of attraction have the same size, the two initial conditions needed to compute  $\tau$  were chosen randomly among the whole state space. Again, the  $\tau \sim 1/r$  behavior for small  $r$  and the  $\tau \propto 2^{N/2}$  behavior for  $r \rightarrow 0.5$  are obtained. Of course we can construct many other models by choosing different coupling functions  $f_i$  for this  $K = 1$  self-correlated case. All the Kauffman models we have explored have shown this kind of behavior under noise.

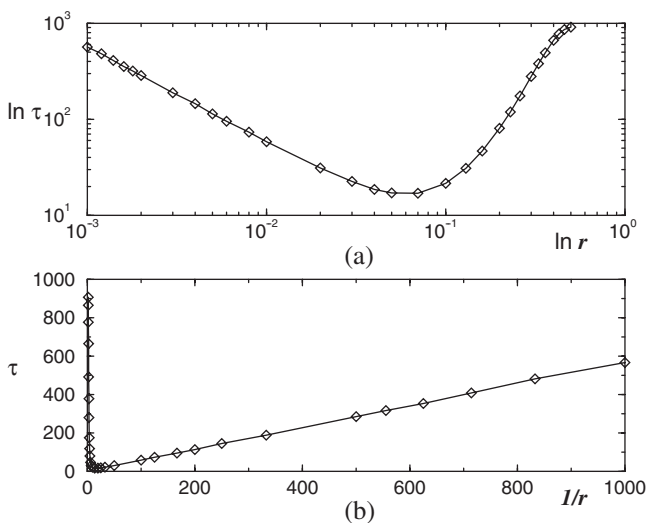


Fig. 6. Average crossing time  $\tau$  ( $\diamond$ ) for a Kauffman lattice with  $N = 20$  and connectivity  $K = 1$  as a function of (a) the noise intensity  $r$  and (b) the inverse of the noise intensity. For this model, every spin is correlated to itself and we choose the Boolean functions in such a way that the whole state space is composed of 8 basins of attraction with equal size. Each point is the average over 10000 realizations of the model.

## 4. THEORETICAL ANALYSIS

### 4.1. Small $r$ Limit

In this region, the main characteristic of average crossing time is that  $\tau_d \sim 1/r$ . The reason for this dependence is that the stochastic dynamics is dominated by one-spin flip events, in the following sense. The probability of a one-spin flip event ( $\sim r$ ) is much larger than the probability of a two-spin flip event ( $\sim r^2$ ). If the probability to jump to a different basin of attraction in a one-spin flip event is significantly different from zero, then the dynamics will be dominated only by this kind of events. Even if it was necessary to flip two spins to jump from one basin to another, this process can be decomposed into two one-spin flip events occurring sequentially, instead of being carried out at once in one two-spin flip event.

As we have shown in Section 3, the  $1/r$  behavior is present in a wide variety of Kauffman models. This in turn, implies that the one-spin flip events dominate the dynamics for small values of the noise. In this subsection, our goal is to derive an expression for the coefficient  $a(K, N)$  for Kauffman nets. To do so, we will make the assumption that the dynamics takes place only in the two largest basins of attraction. Although the  $\tau_d \sim 1/r$  behavior is generally true, as we have found, the preceding assumption is not true for all Kauffman models, especially for those with small values of  $K$ , but as we show below, it becomes more valid as  $K$  increases.

To start the calculation of  $a(K, N)$ , let  $P_{1,2}$  be the probability for jumping from the largest basin to the next largest basin with a one-spin flip event and  $P_{2,1}$  be a similar probability but jumping in the opposite direction.<sup>3</sup> Let us also define  $Q_1$  and  $Q_2$  as the probabilities of remaining in the largest basin and in the next largest one, respectively, after one-spin flip event. Simulations show that for Kauffman nets these probabilities have a slight dependence on  $N$  but a very strong dependence on  $K$ . The result is that  $P_{1,2} + Q_1 \approx P_{2,1} + Q_2 \approx M$ , where  $M$  is approximately constant for all values of  $K$  and  $M > 0.92$  (see Fig. 7).

However, the dynamics depends not only on the total sum  $M$  but also on the particular values of  $P_{1,2}$ ,  $Q_1$ ,  $P_{2,1}$  and  $Q_2$ . For small values of  $K$ , both  $P_{1,2}$  and  $P_{2,1}$  are very small and comparable with  $(1 - M)$ . So, even though  $M$  is large, the interaction between the two largest basins is weak in the sense that the probability of jumping into smaller basins is of the same order as  $P_{1,2}$  and  $P_{2,1}$ . Therefore, for small values of  $K$  the smaller basins play a significant role in the dynamics of the system. The above can be seen

<sup>3</sup> By definition, the ratio of  $P_{1,2}$  and  $P_{2,1}$  is strictly the inverse of the ratio of the size of the largest basin to the next largest one in one realization.

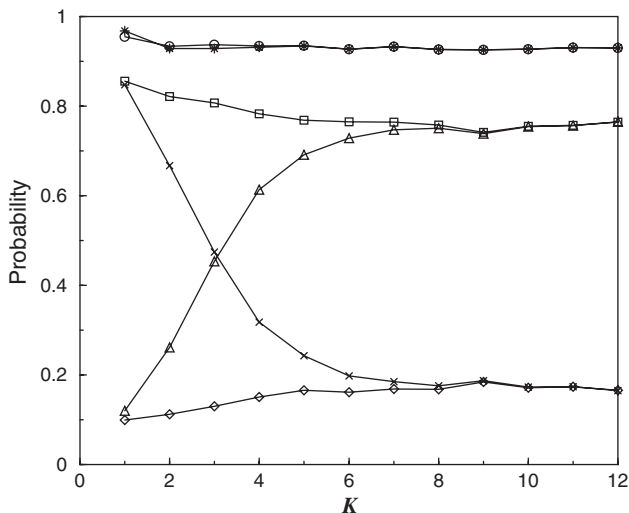


Fig. 7. Plot of the probabilities  $P_{1,2}$  ( $\diamond$ ),  $P_{2,1}$  ( $\triangle$ ),  $Q_1$  ( $\square$ ) and  $Q_2$  ( $\times$ ) as functions of  $K$ , for a Kauffman net with  $N = 12$ . Also shown is  $M$  as a function of  $K$ , obtained as  $M = P_{1,2} + Q_1$  ( $*$ ), and as  $M = P_{2,1} + Q_2$  ( $\circ$ ). Note that even though  $M$  is a constant for all values of  $K$ , the probabilities  $P_{1,2}$  and  $P_{2,1}$  are rather small for small values of  $K$ .

in Fig. 7, in which the probabilities  $P_{1,2}$ ,  $P_{2,1}$ ,  $Q_1$ ,  $Q_2$ , and the sum  $M$  are plotted as functions of  $K$ . From this figure it is apparent that the two largest basins of attraction are the dominant ones for large values of  $K$  (say  $K \geq 5$ ). The closeness of  $M$  to 1 means that a trajectory will seldom jump into a basin other than the two largest ones with only one-spin flip event. In view of this result, in some of the arguments below we will assume that  $K$  is sufficiently large so that the dynamics takes place only in the two largest basins of attraction.

With the information about these probabilities, we can give an approximate calculation of  $\tau_d$  as a function of  $r$  for the case in which  $K$  is large. We know that every spin violates the deterministic rule (1) with probability  $r$ . Therefore, the probability of a one-spin flip event is  $Nr$  and consequently the expected time for this event to occur is  $T = 1/(Nr)$ . This is true for all configurations. For sufficiently small values of  $r$ , this expectation time is much longer than the average crossing time for two configurations in the same basin. Hence, once two configurations jump into the same basin, their trajectories meet before the next spin-flip event becomes possible.

There are two cases in which the two trajectories meet after the occurrence of a one-spin flip event at time  $T$ : the configuration in the

largest basin remains in it while the configuration in the next largest basin jumps into the largest one, or vice versa. The above occurs with probability  $(Q_1 P_{2,1} + Q_2 P_{1,2})$ . Similarly we get the probability for the crossing of the two trajectories after one-spin flip events at  $2T$ ,  $3T$ , etc. The average value of  $\tau_d$  is then:

$$\begin{aligned} \tau_d &\approx T \cdot (Q_1 P_{2,1} + Q_2 P_{1,2}) + 2T \cdot (Q_1 Q_2 + P_{1,2} P_{2,1}) \cdot (Q_1 P_{2,1} + Q_2 P_{1,2}) + \dots \\ &= \sum_{m=1}^{\infty} m \cdot T \cdot (Q_1 P_{2,1} + Q_2 P_{1,2}) \cdot (Q_1 Q_2 + P_{1,2} P_{2,1})^{m-1} \\ &= \frac{1}{Nr} \cdot \frac{Q_1 P_{2,1} + Q_2 P_{1,2}}{(1 - Q_1 Q_2 - P_{1,2} P_{2,1})^2} \\ &= \frac{a(K, N)}{r} \end{aligned} \tag{6}$$

where  $a(K, N)$  is explicitly given by

$$a(K, N) = \frac{1}{N} \frac{Q_1 P_{2,1} + Q_2 P_{1,2}}{(1 - Q_1 Q_2 - P_{1,2} P_{2,1})^2} \tag{7}$$

In the above derivation, which is true for the case in which  $K$  is large, we have ignored the time  $b(K, N)$  it takes for two trajectories to cross after they have jumped into the same basin. Figure 8 shows the coefficient  $a(K, N)$  obtained from Eq. (7) and from simulation, for different values of  $K$  in a Kauffman net with  $N = 12$ . It can be seen that the simulation and the theoretical result agree very well for  $K \geq 5$ . It is worth emphasizing that for small values of  $K$  and other Kauffman models where the two largest basins don't have such dominance, the effect of other basins besides the largest and next largest ones has to be considered to perform an accurate derivation for the coefficient  $a(K, N)$ .

## 4.2. Large $r$ Limit

When  $r$  acquires its maximum value 0.5, the barriers between different attractors vanish and the dynamics transforms into a random mapping of the state space into itself.<sup>(11,12)</sup> In this limit, the crossing times  $\tau_s$  and  $\tau_d$  become indistinguishable and we will refer to both of them simply as  $\tau$ . To understand the limit  $r \rightarrow 0.5$  we will first give a simple "birthday-problem" argument to obtain the order of magnitude of  $\tau$ . Then we will proceed to a

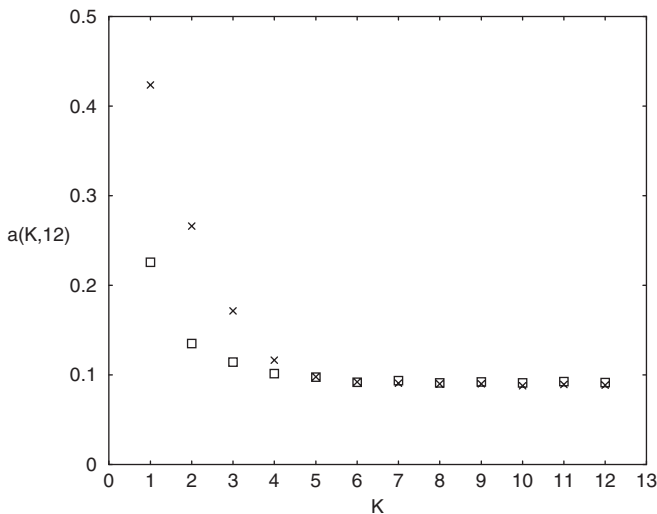


Fig. 8. The coefficient  $a(K, N)$  in Eq. (3) for different values of  $K$  for a Kauffman net with  $N = 12$ . ( $\times$ ) is the result obtained from simulations by sampling the whole state space. ( $\square$ ) is the result obtained from the theoretical result Eq. (7).

more elaborate analysis to obtain an approximate expression for  $\tau$  as a function of  $r$ , valid for  $r$  close to 0.5.

Imagine two walkers moving at random through a space of dimension  $\Omega = 2^N$ . They go through a number of steps  $n = 1, 2, 3, \dots$ . As each step is completed, they have a total number of chances  $C_n$  on landing on some place previously covered by the other walker. At the first step we could have the two walkers at identical positions. Thus,  $C_1 = 1$ . At the second step,  $C_2 = 3 + C_1$  since each can land on the original position of the other or they can both land at precisely the same place. After  $n$  steps  $C_n = C_{n-1} + 2n + 1 = n^2$ . For large  $\Omega$  and small  $n$ , the probability of having collided with the path is then of order  $p_n \approx C_n/\Omega$ . The average time for crossing is then roughly given by the  $n$ -value for which  $p_n$  becomes of order unity, so that  $n^2$  is of order  $\Omega$  or  $n = O(\Omega^{1/2})$ . Therefore, the crossing time  $\tau$  satisfies  $\tau \propto \Omega^{1/2}$ .

To derive a more precise functional relation between  $\tau$  and  $r$  we have to compute the probability  $p_c(t)$  for two trajectories  $\{\Sigma_0, \Sigma_1, \dots, \Sigma_\tau\}$  and  $\{\tilde{\Sigma}_0, \tilde{\Sigma}_1, \dots, \tilde{\Sigma}_\tau\}$  to cross at time  $\tau$ . In order to do that, we have to have first the probability  $p$  for two configurations  $\Sigma_t$  and  $\tilde{\Sigma}_{\tilde{t}}$  to be the same (note that  $t$  and  $\tilde{t}$  might be different). Let  $S_i(t-1)$  be in  $\Sigma_{t-1}$  and  $\tilde{S}_i(\tilde{t}-1)$  be the corresponding spin in  $\tilde{\Sigma}_{\tilde{t}-1}$ . Since these spins are in the same position (each

in its respective configuration), the deterministic rule  $f_i$  they obey is the same. Notice that the dynamical equation (2) can be written as

$$S_i(t+1) = \begin{cases} f_i & \text{with probability } 1-2r, \\ \text{evolve randomly} & \text{with probability } 2r. \end{cases} \quad (8)$$

From this expression it follows that the probability for  $S_i(t-1)$  and  $\tilde{S}_i(\tilde{t}-1)$  to evolve according to the deterministic rule  $f_i$  is  $(1-2r)^2$ . Let us denote by  $p_1$  the probability that  $S_i(t) = \tilde{S}_i(\tilde{t})$  when both spins are updated according to the deterministic rule  $f_i$ . To calculate  $p_1$  we follow the annealed approximation introduced by Derrida and Pomeau,<sup>(6)</sup> which leads us to the following two possibilities:

(1) The  $K$  inputs of  $S_i(t-1)$  and  $\tilde{S}_i(\tilde{t}-1)$  are the same, which occurs with probability  $1/2^K$ . When this happens,  $S_i(t) = \tilde{S}_i(\tilde{t})$  with probability 1.

(2) At least one of the inputs is different, which occurs with probability  $(1-1/2^K)$ . In this case, if the evolution rules  $f_i$  are assigned in a sufficiently random way, there is a probability of  $1/2$  that  $S_i(t) = \tilde{S}_i(\tilde{t})$ .

From the above it follows that

$$p_1 = (1-2r)^2 \left[ \frac{1}{2^K} + \left(1 - \frac{1}{2^K}\right) \cdot \frac{1}{2} \right]$$

On the other hand, the probability  $p_2$  that  $S_i(t) = \tilde{S}_i(\tilde{t})$  when the evolution rule  $f_i$  is violated in one or both of the configurations, is simply given by

$$p_2 = [1 - (1-2r)^2] \cdot \frac{1}{2}$$

Combining the values of  $p_1$  and  $p_2$  given above, the probability  $p$  for both configurations  $\Sigma_i$  and  $\tilde{\Sigma}_{\tilde{i}}$  to be equal is

$$\begin{aligned} p &= \left\{ (1-2r)^2 \left[ \frac{1}{2^K} + \left(1 - \frac{1}{2^K}\right) \cdot \frac{1}{2} \right] + [1 - (1-2r)^2] \cdot \frac{1}{2} \right\}^N \\ &= \frac{1}{2^N} \cdot \left\{ 1 + \frac{1}{2^K} \cdot (1-2r)^2 \right\}^N \end{aligned} \quad (9)$$

If  $q(t)$  is the probability that the two trajectories have not yet crossed at time  $t$ , then  $p_c(t)$ , the probability for the two trajectories to cross at time  $t$ , is given by

$$p_c(t) = q(t-1) - q(t) \quad (10)$$



The two trajectories are still separated at time  $t$  if none of the configurations  $\{\Sigma_0, \Sigma_1, \dots, \Sigma_t\}$  is equal to any of the configurations  $\{\tilde{\Sigma}_0, \tilde{\Sigma}_1, \dots, \tilde{\Sigma}_t\}$ . The probability for this to happen is

$$q(t) = (1-p)^{(t+1)^2}$$

Substituting this value of  $q(t)$  into equation (10) we get

$$p_c(t) = (1-p)^{t^2} - (1-p)^{(t+1)^2} \tag{11}$$

Therefore, the average crossing time  $\tau = \sum_{t=1}^{\infty} t \cdot p_c(t)$  is given by

$$\begin{aligned} \tau &= \sum_{t=1}^{+\infty} t \cdot [(1-p)^{t^2} - (1-p)^{(t+1)^2}] \tag{12} \\ &\approx \int_0^{+\infty} -t \frac{d(1-p)^{t^2}}{dt} dt \\ &= \frac{1}{2} \sqrt{\frac{\pi}{-\ln(1-p)}} \end{aligned}$$

Expanding the logarithm in the above equation around  $p = 0$ , and retaining only the terms up to the the first order, we finally get

$$\tau \approx \frac{\sqrt{\pi}}{2} \left[ \frac{2}{1 + \frac{1}{2^k} \cdot (1-2r)^2} \right]^{N/2} \tag{13}$$

It can be seen that Eq. (13) is consistent with the ‘‘birthday-problem’’ argument for the case  $r = 0.5$ . When  $r$  is not exactly 0.5, we do not have a simple birthday problem because the coupling between different elements, and consequently the functions  $f_i$ , still play a role in the dynamics. However, it is clear from the above equation that the problem can be viewed as a birthday problem with an effective state space  $\Omega_{\text{eff}} = \left[ \frac{2}{1 + (1-2r)^2 / 2^k} \right]^{N/2}$ .

Figure 9 compares the theoretical result (13) with the numerical simulation for  $K = 1$  and  $K = 5$ . As can be seen, the analytic result approximates very well the numerical data in the region of  $r$  close to 0.5. In this region the annealed approximation holds because the noise breaks the correlations between the spins. However, for small values of the noise those correlations are important and cannot be neglected. We therefore do not expect agreement between the numerical and theoretical results for small values of  $r$  since in this region the annealed approximation is not longer valid.

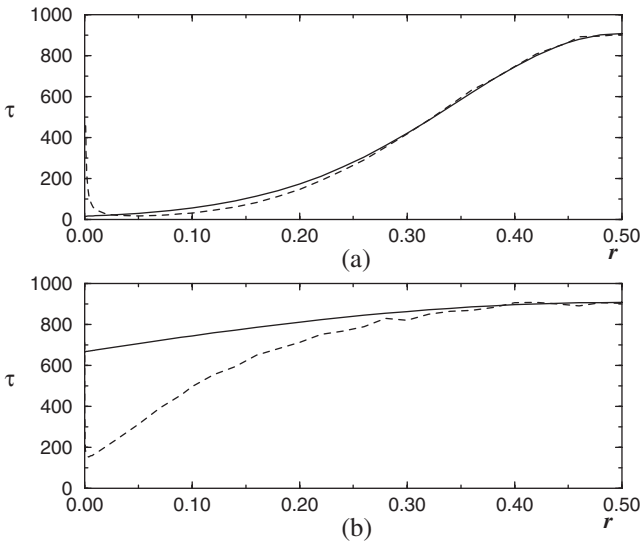


Fig. 9. Average crossing time  $\tau$  as a function of  $r$  for two Kauffman nets with  $N = 20$  and connectivities (a)  $K = 1$  and (b)  $K = 5$ . In both graphs the dashed curve is the result of the numerical simulation for  $\tau_d$ , whereas the solid line is the plot of the analytic expression (13).

## 5. CONCLUSIONS

We have considered the effect of external perturbations (noise) in the dynamics of the Kauffman model. The behavior of both, the Kauffman net and the Kauffman lattice under the influence of noise is very similar, even though these models might have a quite different structure in their basins of attraction. In this sense, the response of the Kauffman models to the effect of noise can be considered as a very robust property.

In the limit  $r \rightarrow 0$ , the most important property is the  $1/r$  behavior of the crossing time  $\tau_d$ , which has been always present in the Kauffman models we have studied so far. This  $1/r$  behavior is a consequence of the fact that, for small values of the noise, the dynamics is dominated by one-spin flip events. An approximate equation relating  $\tau_d$  and  $r$  was obtained by taking into account the fact that, for large values of the connectivity, most of the dynamics takes place in the largest and next largest basins of attraction.

In the second limit  $r \rightarrow 0.5$ , the barriers between different attractors disappear and the dynamics transforms into a random mapping of the state space into itself. As a consequence,  $\tau_s$  and  $\tau_d$  become equal. In the case in which  $r = 0.5$ , the crossing time between the two trajectories can be seen as

the solution of a “birthday problem” in a space of size  $\Omega = 2^N$ . For other values of  $r$ , but still close to 0.5, the correlations between spins have to be taken into account, which have the effect of reducing the size of the region of the state space explored by the dynamics.

Between these two limit cases for the noise, there is a minimum in the value of  $\tau_d$  as a function of  $r$ . In a loose sense, this minimum could be interpreted as the result of a “competition” between the randomness generated by the noise, which tends to homogenize the state space by diminishing the barriers across different attractors, and the deterministic dynamics, which tends to confine two trajectories within the same basin. To analyze this region it would be necessary to consider multiple-spin flip events as well as long-time step correlations.

The results and techniques presented in this work could be extended to other systems acting under the influence of noise in order to provide them with a robust characterization.

## ACKNOWLEDGMENTS

This work was supported in part by the MRSEC Program of the National Science Foundation under award number 9808595, and by the NSF DMR 0094569. We also thank to the Santa Fe Institute of Complex Systems for partial support through the David and Lucile Packard Foundation Program in the Study of Robustness.

## REFERENCES

1. S. A. Kauffman, Metabolic stability and epigenesis in randomly constructed nets, *J. Theor. Biol.* **22**:437–467 (1969).
2. M. Aldana-González, S. Copersmith, and L. Kadanoff, Boolean dynamics with random couplings, *Springer Applied Mathematics Series*, to appear, see also <http://arXiv.org/abs/nlin.AO/0204062>.
3. S. Bilke and F. Sjunnesson, Stability of the Kauffman model, *Phys. Rev. E* **65**:016129 (2001).
4. E. N. Miranda and N. Parga, Noise effects in the Kauffman model, *Europhys. Lett.* **10**:293–298 (1989).
5. O. Golinelli and B. Derrida, Barrier heights in the Kauffman model, *J. Phys.* **50**:1587–1601 (1989).
6. B. Derrida and Y. Pomeau, Random networks of automata—a simple annealed approximation, *Europhys. Lett.* **1**:45–49 (1986).
7. B. Derrida and G. Weisbuch, Evolution of overlaps between configurations in random boolean networks, *J. Phys.* **47**:1297–1303 (1986).
8. H. J. Hilhorst and M. Nijmeijer, On the approach of the stationary state in Kauffmans random boolean network, *J. Phys.* **48**:185–191 (1987).

9. B. Derrida and H. Flyvbjerg, Distribution of local magnetizations in random networks of automata, *J. Phys. A* **20**:L1107–L1112 (1987).
10. B. Derrida, Valleys and overlaps in Kauffman model, *Philos. Mag. B* **56**:917–923 (1987).
11. B. Harris, Probability distributions related to random mappings, *Ann. Math. Statist.* **31**:1045–1062 (1960).
12. B. Derrida and H. Flyvbjerg, The random map model: A disordered model with deterministic dynamics, *J. Phys.* **48**:971–978 (1987).